

OPTIMIZATION APPROACHES IN DESIGN FOR ADDITIVE MANUFACTURING

Rosso, Stefano; Savio, Gianpaolo; Uriati, Federico; Meneghello, Roberto; Concheri, Gianmaria

Università degli Studi di Padova, Italy

ABSTRACT

Nowadays, topology optimization and lattice structures are being re-discovered thanks to Additive Manufacturing technologies, that allow to easily produce parts with complex geometries.

The primary aim of this work is to provide an original contribution for geometric modeling of conformal lattice structures for both wireframe and mesh models, improving previously presented methods. The secondary aim is to compare the proposed approaches with commercial software solutions on a piston rod as a case study.

The central part of the rod undergoes size optimization of conformal lattice structure beams diameters using the proposed methods, and topology optimization using commercial software tool. The optimized lattice is modeled with a NURBS approach and with the novel mesh approach, while the topologically optimized part is manually remodeled to obtain a proper geometry. Results show that the lattice mesh modelling approach has the best performance, resulting in a lightweight structure with smooth surfaces and without sharp edges at nodes, enhancing mechanical properties and fatigue life.

Keywords: Additive Manufacturing, Optimisation, Case study, Lattice structures, Modeling approaches

Contact:

Rosso, Stefano
University of Padova
Department of Management and Engineering
Italy
stefano.rosso.3@phd.unipd.it

Cite this article: Rosso, S., Savio, G., Uriati, F., Meneghello, R., Concheri, G. (2019) 'Optimization Approaches in Design for Additive Manufacturing', in *Proceedings of the 22nd International Conference on Engineering Design (ICED19)*, Delft, The Netherlands, 5-8 August 2019. DOI:10.1017/dsi.2019.85

1 INTRODUCTION

Nowadays, optimization is a fundamental phase during the development of a new product; finding the right moment when to start to optimize is essential to save time, money and obtain an innovative product. In the past decades, optimization was performed as the third phase out of four of the design process (Kirsch, 1993): after the formulation of functional requirements and the conceptual design stage, the optimization step is conducted in an iterative-intuitive way, based on trial and error. This approach tends to be time-consuming as often the first guess does not satisfy the requirements, and other solutions have to be designed and tested, in an iterative process. If, instead, computational design synthesis (Chakrabarti, 2002) is used, the tasks needed to obtain a solution can be divided in four main steps: representation, where a mental model of the object is created, generation, where the object is created, evaluation, where an analysis is performed to see how well the part meets the design goals and constraints, and guidance, in which feedback on improvements to the design for the next iteration is given (Cagan *et al.*, 2005); generation, evaluation and guidance phases are iteratively repeated until a final design is obtained. In design synthesis, optimization can occur during representation and generation phases, where the design has not yet been refined to a specific topology. Usually, stochastic methods are applied, since it is not mandatory to find exact global optima, but it is possible to explore different design that can generate suboptimal designs that satisfy the designer's needs (Shea and Cagan, 1997). Applications of stochastic methods were proposed by Shea, Aish and Gourtovaia (2005), where a generative structural design system including structural topology and shape annealing (STSA) method is combined with an associative modeling system, and by Shea and Smith (2006) where STSA is applied for improving full-scale transmission tower design. Since stochastic methods are iterative processes, they could require lot of time and computational resources, according to the number of iteration and variables of the problem. A similar approach, called Simulation-Driven Design or Optimization-Driven Design, has been adopted by both academic researchers (Sellgren, 1999; Koziel and Ogurtsov, 2014) and commercial software (Altair, 2018). Moving up and embedding the optimization in the first concept and design definition, the resulting shape will drive the following validation and production phases in a faster way, with no need for further iterations.

Among all the types of optimization, structural optimization aims to find the best way to organize material in a structure, according to loads and boundary conditions applied on the part. Objectives of the optimization can be mass reduction, stiffness maximization and resonant frequencies. Structural optimization can be mainly arranged into three classes (Bendsoe and Sigmund, 2013).

1. *Size optimization*: it deals with the optimization of the dimensions, which involve, for example, the cross sections of trusses inside a structure and/or thicknesses of plates.
2. *Shape optimization*: it deals with the optimization of the shape of boundaries of the structure; it affects not only the external boundaries but also the shape of potential internal voids.
3. *Topology optimization*, in which material is arranged in order to find the best distribution under a set of boundary conditions.

All the structures and shapes resulting from the aforementioned optimization and modeling techniques present really complicated geometries, difficult and sometimes impossible to produce with conventional manufacturing technologies. Additive Manufacturing (AM) technologies, instead, due to their layer-by-layer manufacturing approach, allow for the production of complex shapes without necessary increasing production costs and times (Holmström *et al.*, 2010). In their work, Brackett, Ashcroft and Hague (2011) presented opportunities, and practical difficulties as well, of topology optimization for AM. In (Rosen, 2016) a review of synthesis methods for AM can be found; in particular, topology optimization methods, codes, commercial software and research issues are reported. Another thorough review that summarizes the state of the art topology optimization methods and exposes current challenges and opportunities in the AM field can be found in (Liu *et al.*, 2018). Common issues and limitations are the integration of AM process constraints during topology optimization, the addressing of multi-scale modeling, multiple loading conditions and local constraints, multiple materials, robustness with respect to variations and computational efficiency of the methods. Zegard and Paulino (2016) addressed the post-processing phases needed to allow a topologically optimized part to be additively manufactured. In this scenario, lattice structures are receiving increasing attention. In addition to the fact of being lightweight, lattices present other interesting properties: they are stiff in relation to their low mass, they are good energy absorbers thanks to the possibility to undergo large deformations, good acoustic insulators thanks to the internal

porosity and good heat exchangers due to their large surface area (Savio *et al.*, 2018). Moreover, structural optimization has been widely applied to lattice design. In (Ning and Pellegrino, 2012), topology optimization methods are divided in continuum methods, such as Solid isotropic material with penalization (SIMP) method (Bendsøe, 1989; Bendsøe and Sigmund, 1999) and homogenization method, and discrete methods, such as ground-structure based methods and shape-grammar methods; both of the categories present some limitations, so the authors proposed an implicit representation of the structural topology, where the microstructure is defined by a continuous variable, i.e. the size distribution field. More, an optimization loop running under a genetic algorithm is implemented to optimize the size and the topology of a lattice structure. Nessi and Stanković (2018) used the Superformula, an extension of the Superellipse, to obtain a design domain in which a tetrahedral meshing technique was applied to generate the topology of a lattice structure; the size of the struts of the lattice resulting from the edges of the tetrahedral mesh was then optimized using a finite element analysis, given a set of loads and boundary conditions. More, Stanković *et al.* (2015) developed a generalized optimality criteria method for the optimization of lattice structures, including DfAM constraints and exploiting multi material possibilities offered by these technologies; results show that multi material lattices outperform single material ones. Also, the density map resulting from topology optimization can be used to proportionally assign the dimension of the beams or the size of the cells (Han and Lu, 2018; Wang *et al.*, 2018).

The aim of this work is twofold: proposing an extension of a previous lattice structure modeling method to conformal lattices, and comparing it with other commercial approach. Different geometric modeling approaches and structural optimizations methods are presented, both developed by the group of research and available in commercial software, and applied to a piston rod. A conformal wireframe is modeled with a novel approach that uses the curvature of the profile arc curves of the central part of the rod; then, the beams of a lattice structure built around the conformal wireframe are dimensioned with a size optimization algorithm; the optimized lattice is then modeled by a Non-Uniform Rational B-Splines method (Savio, Meneghello and Concheri, 2017) and a mesh method (Savio, Meneghello and Concheri, 2018) with a new feature able to build the mesh faces around nodal points of non-regular lattices. Furthermore, the central part of the rod is topologically optimized and the geometries are remodeled and structurally analysed using commercial software. The results obtained by the three approaches (NURBS method, mesh method and topology optimization method) are finally compared. Outcomes highlight that the mesh modeling method is able to efficiently create conformal lattices with enhanced fatigue behaviour.

2 TOOLS AND METHODS

Sections 2.1 and 2.2 present an improvement of a methods previously developed by Savio, Meneghello and Concheri (2018), introducing the possibility of modeling conformal lattice structures. Section 2.3 deals with an alternative design procedure consisting in topology optimization followed by a manual remodeling and a structural analysis of the part.

The previous method has advantages, such as low computational resources requirements, it is fast and enhances the fatigue behaviour of the parts, but, at the same time, lacks in extension of the available single cells database and does not allow for the modeling of conformal lattices. In conformal structures the geometry and the size of the cells can be different inside the part in order to adapt (i.e. conform) to the external shape of the model: this feature eliminates weakness at boundaries and provides stiffness and resistance to the entire model (Wang, 2005). This new feature increases the field of application of the method, allowing to address filling situations where it is not possible to accept lattice structures with regular repetitions of uniform lattices. In Figure 1 a flow chart regarding the proposed method is presented, highlighting the main novel contribution.

The size optimization was performed in Rhinoceros 6 (Robert McNeel & Associates), using the graphical algorithm editor Grasshopper and Karamba3D as finite element (FE) solver for beams and shells, and an ad-hoc iterative process in Python programming language. The optimization follows these steps:

- A part is given as input and a lattice structure wireframe is created inside, according to the cell type and minimum dimension; the lattice structure created is a conformal one, so the geometry and the size of the cells can adapt (i.e. conform) to the external shape of the model;

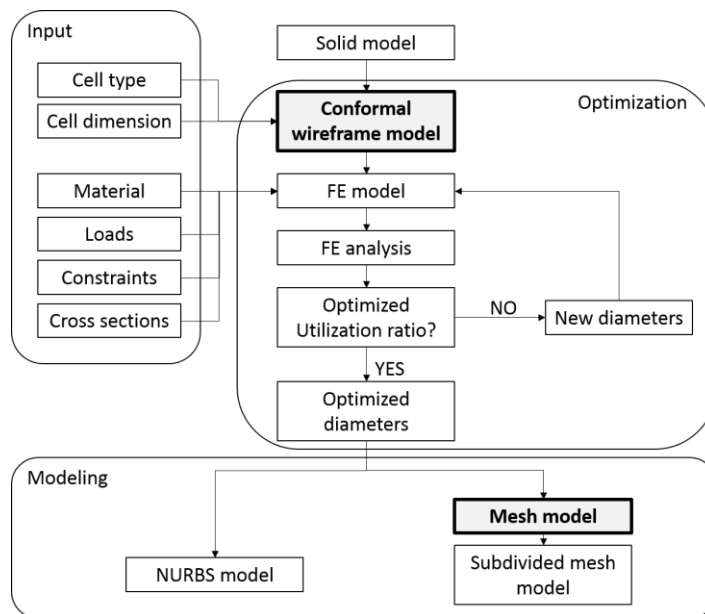


Figure 1. Flow chart of the proposed method.

- A FE beams model is obtained from the wireframe applying the boundary conditions: material, loads, constraints, initial cross-section equal for each beam.
- A FE analysis (FEA) is performed and the utilization of each beam, similar to the ratio between the maximum Von Mises stress at a beam and the admissible stress, is computed. An iterative variation of the beams diameter is carried out until the utilization ratio of each beam is inside a target range. An upper and lower bound for beam dimension are defined to allow the beam to be manufactured (i.e. the beam diameter has to be bigger than the lower bound), and to not interfere with the nearby beams (i.e. the beam diameter has to be smaller than the upper bound).

Once the FE model has been optimized, the lattice structure is modeled adopting two different boundary representation approaches: Non-Uniform Rational B-Splines (NURBS) modeling and mesh modeling.

Adopting NURBS modeling, a cylinder having the optimized diameter and spherical caps is constructed around each line of the model; Boolean union over the capped cylinders is then performed to obtain the lattice structure. The resulting model presents a lot of sharp edges that cause stress concentration at nodal points and mechanically weaken the structure.

Using mesh modeling, an 8-faces mesh is modeled around each beam, assuming a double truncated pyramidal shape. At the middle of the beam, the optimized diameter dimension is adopted, while at the ends, where the beam approaches the nodes, the diameter dimension of the biggest beam arriving at the node is used, to avoid issues in the mesh model reconstruction.

Catmull-Clark subdivision surface algorithm is finally adopted (Catmull and Clark, 1978). With Catmull-Clark subdivision, starting from a quadrilateral mesh, the initial vertices are iteratively averaged following the subdivision rule, splitting into four each quad face and resulting in a smooth surface; this algorithm produces a surface with continuity in curvature (C2 surface), except at extraordinary vertices where they are C1 (Catmull and Clark, 1978; Zorin, 2000).

2.1 Conformal wireframe model

Conformal wireframes can be obtained adopting morphing algorithms to map a regular wireframe on a specific shape, but the tested implementation provided cells with bigger surface area at vertex. Instead, exploiting curvature information guarantees a better control on the final cells.

Starting from 4 boundary profiles arcs (Figure 2a), conformal wireframe is modeled according to the following steps:

- the line connecting the mid-point of the upper and lower profiles is created and divided by the minimum cell size value, obtaining the number of arcs along this direction, n ;
- the curvatures of the upper and lower profile arcs are extracted; these two values are linearly interpolated obtaining n intermediate curvature;

- the line connecting the mid-point of the upper and lower profiles is created and subdivided in n points (Figure 2b);
- n new arcs are obtained imposing the passage on the n subdivision points; the centres lays on an extension of the previously created line and the radius is obtained from the n -th interpolated curvature value (Figure 2c);
- same passages are applied to the left and right profile arcs and the complete wireframe is obtained (Figure 2d).

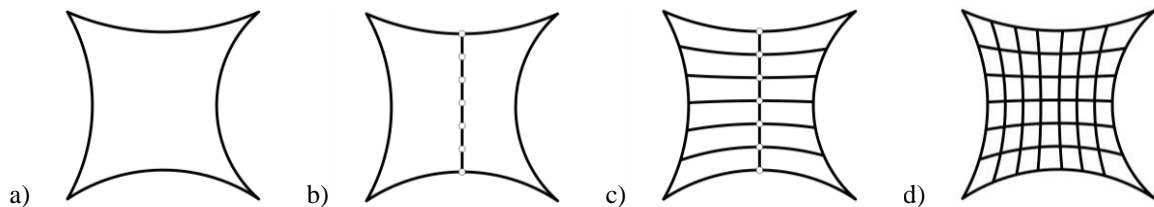


Figure 2. Conformal wireframe creation: a) starting profile arcs, b) arc mid-point line subdivision, c) one-direction wireframe, d) final wireframe.

2.2 Lattice structure mesh modeling

Since the lattice structure is conformal, it is likely to have beams at nodes that are not orthogonal with respect to each other. In order to model a mesh around the wireframe, the following operations are executed:

- cylinders are built around the wireframe model and the intersections points of cylinders approaching the same node are computed; these points will be the vertexes of the mesh; the value of the diameters of cylinders approaching the same node equal to the biggest diameter value obtained from the size optimization (Figure 3a);
- 4 lines linking two nodes are obtained connecting the previously found intersections;
- at the mid-point of each line, new vertexes are obtained and repositioned according to the values of the optimized diameters of the beams (Figure 3b);
- an 8-faces mesh is modeled around each beam, connecting the 12 vertexes, assuming a double truncated pyramidal shape (Figure 3c).

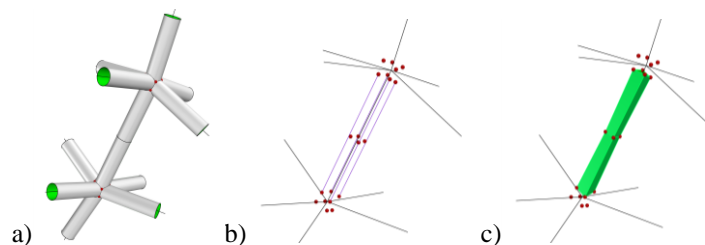


Figure 3. Mesh modeling at nodal points: a) cylinders intersections vertexes, b) mid vertexes, c) mesh beam model.

2.3 Topology optimization

Another possible structural optimization approach is given by topology optimization. With TO, a specific zone of the product, called “design space”, is defined. It is recommended to simplify as much as possible the geometry, avoiding fillets, chamfers, and pocket holes, to let the optimization work better. Then, an optimization algorithm distributes the material on the design space according to loads and constraints. The goal of the optimization is usually to maximize the stiffness, imposing a desired reduction of mass, varying the density element by element, which is related to mechanical properties. As a results, a density map is obtained, which is contoured to a specific level of density (threshold), obtaining a mesh surface. The optimized mesh of the design space is taken as an “inspiration” to the further modeling of the part in a CAD tool, often operating manually. Consequently, considering the manual remodeling procedure, a FEA is needed to verify that the stress condition is respected.

Topology optimization is performed in SOLIDWORKS® 2018 Student Edition by Dassault Systemes, with the plugin SOLIDWORKS® Simulation, based on SIMP method. The optimized mesh is

remodeled in Evolve® software by Altair Engineering, Inc., and the remodeled part is then analysed in ANSYS® Workbench 2019 R1, by ANSYS, Inc.

3 RESULTS AND DISCUSSION

3.1 Case study

The case study presented in this work is a piston rod, currently produced with a pressure die-casting process in aluminum EN AC-46100 (AlSi11Cu2Fe); the properties of the material are presented in Table 1. Overall dimensions are shown in Figure 4a.

Table 1. Aluminum EN AC-46100 (AlSi11Cu2Fe) properties.

| Density | Young modulus | Yield strength | Ultimate Tensile Strength | Poisson ratio |
|------------------------|---------------|----------------|---------------------------|---------------|
| 2700 kg/m ³ | 71 GPa | 140 MPa | 240 MPa | 0.34 |

The piston rod is loaded with an axial traction load of 7.5 kN along z-axis applied to the big rod's end and it is constrained by blocking all the displacements and rotations of the nodes belonging to the inner face of the small rod's end and by blocking the displacements along x and y directions of the nodes belonging to the face of the big rod's end to simulate the higher stiffness of the parts that are not optimized and maintain the original geometries. Figure 4b shows the simplified model of the rod with the design space and boundary conditions. The design space was modelled starting from the ZX plane; the arc curve at the big rod's end and the semicircle curve at the small rod's end were extracted; the profile was completed with two symmetric arcs, imposing tangency both at start and at end of the curve. On the YZ plane, two symmetrical arcs were modeled to connect the two rod's ends; tangency was imposed at the big rod's end connection and position in the small.

In order to compare different methods, the optimization and modeling approaches were applied only to the central part of the connecting rod.

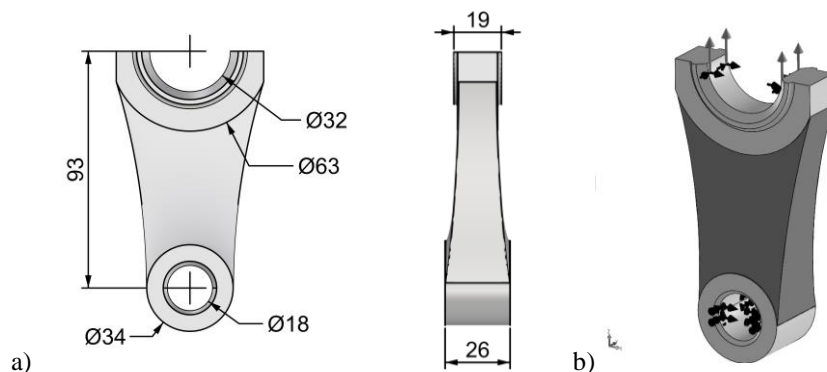


Figure 4. Piston rod: a) overall model dimensions, b) design space (dark grey), loads and constraints.

3.2 Size optimization of the lattice structure

First, the central part of the piston rod was filled with a wireframe representing a conformal lattice structure with a simple cubic unit cell of minimum length equal to 3 mm, following the procedure in Section 2.1 (Figure 5).

The FE model was set-up inside Grasshopper with Karamba3D plugin; loads and constraints previously defined were directly applied at the nodes of the beams placed at the interface between the central part and the big and small rod's ends; since the loads are applied to the nodes, the value of 7.5 kN was equally distributed in each node. The target utilization ratio was set to $(90 \pm 1) \%$ with respect to the yield strength. Upper and lower bound for beams diameter were defined 1.5 mm and 0.5 mm, respectively. Figure 6 shows the distribution of the utilization ratio across the optimized lattice. The results coming from the size optimization, i.e. the optimized beams diameter, were used to model the lattice structure.

Figure 7a shows the piston rod with the central part filled with the optimized lattice structure modeled with NURBS surfaces. A lot of sharp edges can be found in the structure where smaller diameter

beams connect at nodes with bigger ones (Figure 7b). Filletting operations would be useful to reduce stress concentration, but due to the model complexity, are quite difficult if not impossible to perform. It is also important to remark that when dealing with complex geometries, such as organic models or lattice structures, NURBS modeling can be unsuitable due to difficulties in operating Boolean unions and due to high computational and memory resources required (Pasko *et al.*, 2011). In order to solve the aforementioned problems, the conformal lattice structure was remodeled adopting the mesh approach presented in Section 2.2, obtaining the part shown in Figure 7c; there is no need of additional filletting operations (see Figure 7d) and it has been showed that structures modeled with a mesh surface subdivision method present better fatigue behavior (Savio *et al.*, 2019).

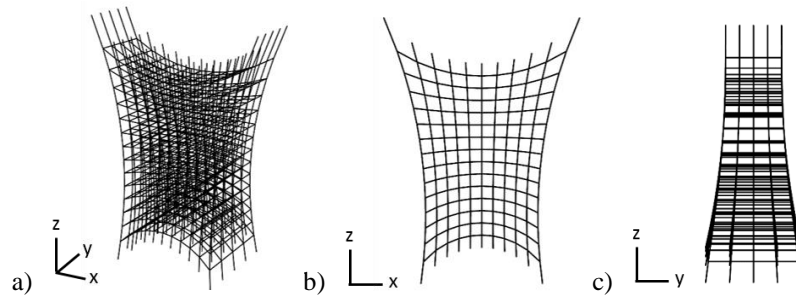


Figure 5. Lattice wireframe: a) perspective view, b) front view, c) side view.

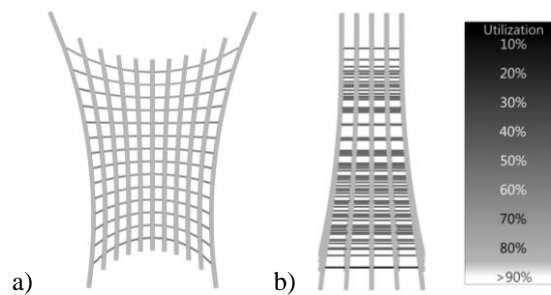


Figure 6. Utilization ratio across the optimized lattice: a) front view, b) side view.

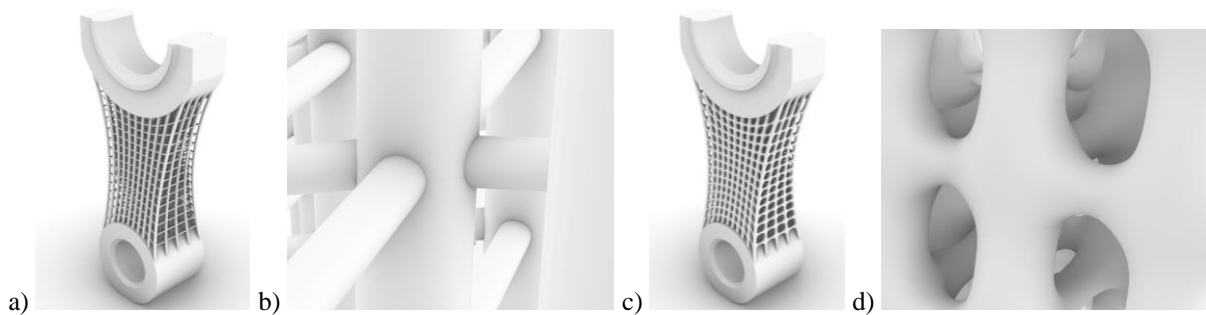


Figure 7. NURBS model: a) piston rod, b) sharp edges at nodal points. Mesh model: c) piston rod, d) smooth surfaces at nodal points due to Catmull-Clark algorithm.

3.3 Topology optimization

The piston rod was topologically optimized using SOLIDWORKS® 2018 Student Edition by Dassault Systemes, with the plugin SOLIDWORKS® Simulation.

First, the rod was remodeled, simplifying all the features. Then, the design space was selected and the loads and constraints were defined. The topology optimization was launched with the goal of “best stiffness to weight ratio” and with the constraint of a final mass equal to 25% of the original part; the mass constraint set to 25% will control the threshold level with which the density map will be contoured. An additional symmetry constraint of the final part with respect to plane YZ and ZX was imposed. The mesh resulting from the optimization was remodeled with a NURBS approach in Altair Evolve® CAD 3D software, exploiting the PolyNURBS modeling feature and the double symmetry of the part. Figure 8 shows the result of the topology optimization (Figure 8a) and the remodeled part (Figure 8b).

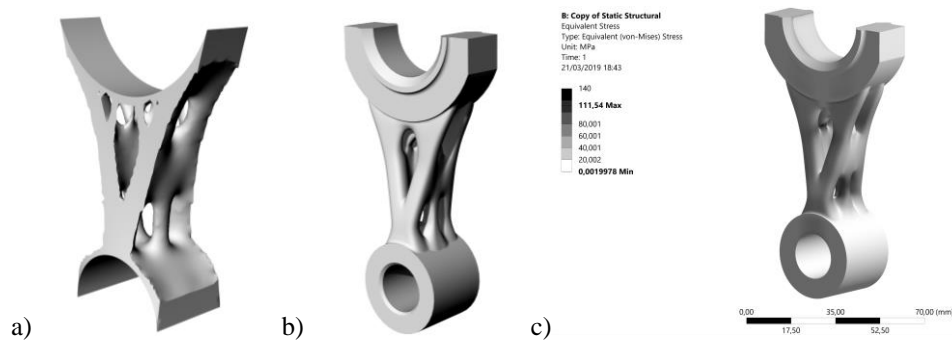


Figure 8. Topology optimization model: a) SOLIDWORKS® Simulation result, b) remodeled part in Altair Evolve, c) equivalent Von-Mises stress.

The remodeled part was then analysed with the Computer Aided Engineering (CAE) software ANSYS® 2019 R1. Boundary conditions, i.e. material, loads, constraints, was set; being the part symmetrical with respect to ZX and YZ plane, this condition was exploited to reduce the computational time. The part was meshed with tetrahedrons element imposing the element minimum size at 0.1 mm in order to obtain at least two elements on the smaller fillet that has a radius of 0.3mm; the element maximum size is 1 mm. The meshing method is patch independent and include automatic refinement in curvature and proximity. Figure 8c shows the analysis results; in particular, equivalent Von-Mises stress distribution is displayed.

3.4 Discussions

Table 2 shows a comparison between the volumes of the simplified piston rod and the ones resulting from the three different optimization and modeling approaches.

Table 2. Volumes of different piston rods.

| | |
|---|--------------------------|
| Simplified piston rod | 73613.32 mm ³ |
| Size optimization + NURBS modelling | 38798.05 mm ³ |
| Size optimization + Mesh modelling | 42791.94 mm ³ |
| Topology optimization + NURBS modelling | 46131.88 mm ³ |

With respect to the simplified piston rod, the size optimized NURBS model, the size optimized mesh model, and the topologically optimized model are respectively 47.29%, 41.87% and 37.33% lighter. During optimization phases, the ends of the piston rod remain untouched; so, a better comparison can be made between the central design space and the optimized geometries (Table 3).

Table 3. Volumes of different modeling approaches for central rod part (design space).

| | |
|---|--------------------------|
| Simplified piston rod | 38778.69 mm ³ |
| Size optimization + NURBS modelling | 3780.30 mm ³ |
| Size optimization + Mesh modelling | 7770.71 mm ³ |
| Topology optimization + NURBS modelling | 11108.95 mm ³ |

From this point of view, the size optimized NURBS model is 90.25% lighter, the size optimized mesh model is 79.96% lighter and the topologically optimized one is 71.35% lighter than the starting simplified central part of the rod.

The NURBS model is the lightest but presents sharp edges at nodal points because of the lack of fillets, that are difficult to perform due to the complexity of the structure; this affects the mechanical behavior, weakening the part. The mesh model, even if it comes from the same size optimization of the NURBS one, is heavier because Catmull-Clark subdivision surface algorithm thickens the beams with smaller diameters when approaching the nodes, resulting in more volume for the structure; but at the same time, the part presents a smooth surface with curvature continuity that guarantees better mechanical properties. Moreover, the modeling approach is automatic. The topologically optimized model is the heaviest of the three optimized models and requires manual remodeling of the mesh resulting from the optimization. However, topology optimization is useful at a conceptual design phase because allows to explore different configurations starting from boundary conditions and simple design spaces, and can be also used imposing technological constraints to produce the part with traditional techniques. Moreover, once remodeled, the topology optimized part needs to be verified

again by a FE analysis, to make sure that the manual remodeling did not introduce weak points inside the part. The results of FE analysis in Figure 8c show that the maximum value for the equivalent Von-Mises stress is 111.54 MPa; since Aluminum AlSi11Cu2Fe has a yield stress of 140 MPa, the connecting rod withstand the applied load with a safety factor (SF) of 1.26, that is close to the 1.1 value used during the size optimization. While during size optimization the SF is imposed as objective of the iterative algorithm with the utilization ratio, in the topologically optimized part SF can only be verified at the end of the process with a FE analysis; also, due to manual remodeling of the part it is difficult to modify the shape in order to obtain the exact SF value.

The beam models were not analysed since it is assumed that size optimization on beam dimension gives a suitable structural verification.

4 CONCLUSIONS

In this work, an improvement of a previous modeling approach was presented, introducing the possibility of modeling conformal lattice structures thus extending the field of application of the design method. More, a piston rod was used as a case study to compare two types of structural optimization: size and topology optimization.

The topologically optimized part is the heaviest of the three models studied; the mesh resulting from TO is coarse and the geometry needs to be remodeled with a CAD software, manually by the user, and validated with FEA. The NURBS model of the lattice structure is the lightest but presents sharp edges at nodal points; this weakens the structure and filleting operations are suggested, but difficult to perform. The mesh model is heavier than the NURBS one but, at the same time, the subdivision method guarantees smooth surfaces, with no need of filleting operations, resulting in an enhanced mechanical behavior and fatigue resistance.

From these observations, the modeling method that uses mesh and subdivision surface algorithm to generate a lattice structure appears to have the best performances. Nevertheless, the method needs to be improved. Indeed, future developments will concentrate on the approaches that deal with the interface between the lattice structure and the connecting rod ends parts (or surfaces/parts to join with, in general) because, by now, the connection still generates sharp edges. More, the conformal wireframe generation method depends on the possibility of simplifying the edges of the design space with four arc curves; alternatively, morphing algorithms can be used to map a regular wireframe on a specific shape, but improvements have to be done to reach a more general method that guarantee a more uniform cell distribution. Attention will be also given to the possibility of modeling different types of single cells, enhancing the method that generates the mesh around nodal points, and also enabling the possibility to suggest the shape of the cell, according to load conditions.

ACKNOWLEDGMENTS

This work was supported by Fondazione Cassa di Risparmio di Padova e Rovigo (CARIPARO).

REFERENCES

- Altair (2018), *Altair Inspire: The Future of Simulation-Driven Design*. Available at: <https://solidthinking.com/product/inspire/> (Accessed: 9 November 2018).
- Bendsøe, M. P. (1989), "Optimal shape design as a material distribution problem", *Structural Optimization*. Springer, Vol 1 No. 4, pp. 193–202.
- Bendsoe, M. P. and Sigmund, O. (2013), *Topology Optimization: Theory, Methods, and Applications*. Springer Science & Business Media.
- Bendsøe, M. P. and Sigmund, O. (1999), "Material interpolation schemes in topology optimization", *Archive of Applied Mechanics*, Vol. 69 No. 9, pp. 635–654. <http://doi.org/10.1007/s004190050248>.
- Brackett, D., Ashcroft, I. and Hague, R. (2011), "Topology optimization for additive manufacturing", in *Proceedings of the Solid Freeform Fabrication Symposium*, Austin, TX. S, pp. 348–362.
- Cagan, J. et al. (2005), "A framework for computational design synthesis: model and applications", *Journal of Computing and Information Science in Engineering*. ASME, Vol. 5 No. 3, p. 171. <http://doi.org/10.1115/1.2013289>.
- Catmull, E. and Clark, J. (1978), "Recursively generated B-spline surfaces on arbitrary topological meshes", *Computer-Aided Design*. Elsevier, Vol. 10 No. 6, pp. 350–355. [http://doi.org/10.1016/0010-4485\(78\)90110-0](http://doi.org/10.1016/0010-4485(78)90110-0).
- Chakrabarti, A. (2002), *Engineering Design Synthesis: Understanding, Approaches, and Tools*.

- Han, Y. and Lu, W. F. (2018), “A novel design method for nonuniform lattice structures based on topology optimization”, *Journal of Mechanical Design*. ASME, Vol. 140 No. 9, pp. 91403–91410. Available at: <http://dx.doi.org/10.1115/1.4040546>.
- Holmström, J. et al. (2010), “Rapid manufacturing in the spare parts supply chain”, *Journal of Manufacturing Technology Management*. Emerald Group Publishing Limited, Vol. 21 No. 6, pp. 687–697. <http://doi.org/10.1108/17410381011063996>.
- Kirsch, U. (1993), *Problem Statement - Structural Optimization: Fundamentals and Applications*, in Kirsch, U. (ed.). Springer Berlin Heidelberg, Berlin, Heidelberg, pp. 1–56. http://doi.org/10.1007/978-3-642-84845-2_1.
- Koziel, S. and Ogurtsov, S. (2014), “Numerically Efficient Approach to Simulation-Driven Design of Planar Microstrip Antenna Arrays by Means of Surrogate-Based Optimization - Solving Computationally Expensive Engineering Problems”, in Koziel, S., Leifsson, L. and Yang, X.-S. (eds). Springer International Publishing, Cham, pp. 149–170.
- Liu, J. et al. (2018), “Current and future trends in topology optimization for additive manufacturing”, *Structural and Multidisciplinary Optimization*, Vol. 57 No. 6, pp. 2457–2483. <http://doi.org/10.1007/s00158-018-1994-3>.
- Nessi, A. and Stanković, T. (2018), “Topology, shape, and size optimization of additively manufactured lattice structures based on the superformula”, in *International Design Engineering Technical Conferences and Computers and Information in Engineering Conference, Volume 2A: 44th Design Automation Conference*. ASME, p. V02AT03A042. <http://doi.org/10.1115/detc2018-86191>.
- Ning, X. and Pellegrino, S. (2012), “Design of lightweight structural components for direct digital manufacturing”, in *53rd AIAA/ASME/ASCE/AHS/ASC Structures, Structural Dynamics and Materials Conference. American Institute of Aeronautics and Astronautics (Structures, Structural Dynamics, and Materials and Co-located Conferences)*, pp. 1–21. <http://doi.org/10.2514/6.2012-1807>.
- Pasko, A. et al. (2011), “Procedural function-based modelling of volumetric microstructures”, *Graphical Models*. Elsevier Inc., Vol. 73 No. 5, pp. 165–181. <http://doi.org/10.1016/j.gmod.2011.03.001>.
- Rosen, D. W. (2016), “A review of synthesis methods for additive manufacturing”, *Virtual and Physical Prototyping*. Taylor & Francis, Vol. 11 No. 4, pp. 305–317. <http://doi.org/10.1080/17452759.2016.1240208>.
- Savio, G. et al. (2018a), “Geometric modeling of cellular materials for additive manufacturing in biomedical field: A review”, *Applied Bionics and Biomechanics*, Vol. 2018, pp. 1–14. <http://doi.org/10.1155/2018/1654782>.
- Savio, G. et al. (2019), “Implications of modeling approaches on the fatigue behavior of cellular solids”, *Additive Manufacturing*. Elsevier, Vol. 25, pp. 50–58. <http://doi.org/10.1016/j.addma.2018.10.047>.
- Savio, G., Meneghello, R. and Concheri, G. (2017), *Optimization of lattice structures for Additive Manufacturing Technologies BT - Advances on Mechanics, Design Engineering and Manufacturing: Proceedings of the International Joint Conference on Mechanics, Design Engineering & Advanced Manufacturing (JCM)*, in Eynard, B. et al. (eds). Springer International Publishing, Cham, pp. 213–222. http://doi.org/10.1007/978-3-319-45781-9_22.
- Savio, G., Meneghello, R. and Concheri, G. (2018b), “Geometric modeling of lattice structures for additive manufacturing”, *Rapid Prototyping Journal*, Vol. 24 No. 2, pp. 351–360. <http://doi.org/10.1108/RPJ-07-2016-0122>.
- Sellgren, U. (1999), “Simulation-driven design: motives, means, and opportunities”. *KTH*.
- Shea, K., Aish, R. and Gourtovaia, M. (2005), “Towards integrated performance-driven generative design tools”, *Automation in Construction*. Elsevier, Vol. 14 No. 2, pp. 253–264. <http://doi.org/10.1016/J.AUTCON.2004.07.002>.
- Shea, K. and Cagan, J. (1997), “Innovative dome design: Applying geodesic patterns with shape annealing”, *Artificial Intelligence for Engineering, Design, Analysis and Manufacturing*. Cambridge University Press, Vol. 11 No. 05, p. 379. <http://doi.org/10.1017/S0890060400003310>.
- Shea, K. and Smith, I. F. C. (2006), “Improving Full-Scale Transmission Tower Design through Topology and Shape Optimization”, *Journal of Structural Engineering*. American Society of Civil Engineers, Vol. 132 No. 5, pp. 781–790. [http://doi.org/10.1061/\(ASCE\)0733-9445\(2006\)132:5\(781\)](http://doi.org/10.1061/(ASCE)0733-9445(2006)132:5(781)).
- Stanković, T. et al. (2015), “A Generalized Optimality Criteria Method for Optimization of Additively Manufactured Multimaterial Lattice Structures”, *Journal of Mechanical Design*. ASME, Vol. 137 No. 11, pp. 111405–111412. Available at: <http://dx.doi.org/10.1115/1.4030995>.
- Wang, C. et al. (2018), “Concurrent topology optimization design of structures and non-uniform parameterized lattice microstructures”, *Structural and Multidisciplinary Optimization*, Vol. 58 No. 1, pp. 35–50. <http://doi.org/10.1007/s00158-018-2009-0>.
- Wang, H. V. (2005), “A unit cell approach for lightweight structure and compliant mechanism”. Georgia Institute Of Technology.
- Zegard, T. and Paulino, G. H. (2016), “Bridging topology optimization and additive manufacturing”, *Structural and Multidisciplinary Optimization*, Vol. 53 No. 1, pp. 175–192. <http://doi.org/10.1007/s00158-015-1274-4>.
- Zorin, D. (2000), “Subdivision zoo”, *Subdivision for Modeling and Animation*, pp. 65–104.